Opt Quant Electron (2016) 48:447
DOI 10.1007/s11082-016-0703-y

Solidification behavior and dendrite structure refinement after LMD in Ti based alloy reinforced by micron- and nano- alumina

Igor Shishkovsky[1,2,3] · **Igor Volyanski**[3] · **Florent Missemer**[2]

Received: 17 July 2016 / Accepted: 15 August 2016 / Published online: 2 September 2016

Abstract The laser metal deposition (LMD) technology with co-axial powder injection was used to fabricate a complex titanium aluminide structure of Ti based alloy reinforced by Al_2O_3 ceramic of micron and nano size particles. The aim of the study was to demonstrate the possibility of producing Ti_xAl_y intermetallic phases in remelting powder mixtures with strain-hardening ceramic inclusions in the course of the single-step LMD process. Besides, relationships between the main laser cladding parameters and the intermetallic phase structures of the built-up objects were studied. In our research we applied optical microscopy, X-ray analysis, microhardness measurement and SEM with EDX analysis of the laser-fabricated intermetallics.

Keywords Laser metal deposition (LMD) · Titanium aluminide · Alumina reinforced titanium matrix composite (ARTMC)

1 Introduction

Titanium based alloys and their intermetallides (γ-TiAl) have a great potential for use in automotive, aerospace and power generation industries (Chen and Wang 2003; Gu et al. 2009a, b). But straightforward approaches to creating these intermetallic phases have run

This article is part of the Topical Collection on Fundamentals of Laser Assisted Micro- & Nanotechnologies.

Guest edited by Eugene Avrutin, Vadim Veiko, Tigran Vartanyan and Andrey Belikov.

✉ Igor Shishkovsky
shiv@fian.smr.ru

[1] Samara Branch, Lebedev Physical Institute of Russian Academy of Sciences, Samara 443011, Russia

[2] DIPI Laboratory, National Engineering School of Saint-Etienne, University of Lyon, 42000 Saint-Etienne, France

[3] Samara State University, Samara 443011, Russia

into some problems, connected with conventional manufacturability and requiring additional post-processing operations (hot-isostatic pressing, ageing, annealing, etc.) for improving desirable properties and receiving demanded shapes. On the other hand, to change the situation with the crack density and the wear performance of the titanium based alloys significantly, fabrication of a metal matrix composites (MMCs) reinforced by titanium carbides and silicides during the laser direct metal deposition (LMD) process can be taken into account (Gu et al. 2011; Krakhmalev and Yadroitsev 2014).

In parallel, Al_2O_3 and TiO_2 powders had been recommended for increasing wear, erosion and corrosion resistance by means of plasma sprayed coating of titanium based alloys (Forouzanmehr et al. 2009; Wang et al. 2009; Chen et al. 2013; Li et al. 2011, 2014). The TiO_2 addition was proved helpful to enhance toughness and wear resistance in comparison with Al_2O_3 coatings. But alumina itself reinforces titanium matrix composites (AR-TMCs) also and has a great potential for γ-TiAl manufacturing with outstanding comprehensive properties (Shishkovsky and Smurov 2012). The micrometer scale of the alumina particulate reinforcements in the TMCs was demonstrated earlier (Forouzanmehr et al. 2009; Wang et al. 2009; Chen et al. 2013; Li et al. 2011, 2014). It was also shown that adding refractory Al_2O_3 to Ti matrix leads to in situ reaction of titanium aluminides intermetallic phase formation because of remelting and releasing of Al. Five mechanisms are known for the intermetallide alloy strengthening, they are a solid-solution, dispersion, grain-boundary, deformation and textural strengthening. The first three ones depend on the alloy nature. The titanium aluminides play role of the hardening mechanism in the TMCs and they are generally explained in terms of the Hall–Petch relationship. Therefore by our opinion, the particle size decreases to nanometer range, the nano-Al_2O_3 fraction reinforced metal matrix composites (nARTMCs) will exhibit interesting properties also.

In the present study, multiphase titanium aluminides were manufactured in situ during the LMD process, by laser remelting of Ti (10, 20, 30 wt%) Al_2O_3 powder mixtures. We compared how the interfacial properties would change due to the difference in composition in case of the μ- and n-ARTMCs. The fabricated ultrafine composites formed in situ were investigated to discover the correlation of microstructures and phase constitution with the composition of the precursor powders. Special attention was paid to dissolution behavior and cracking susceptibility of the fabricated microstructure, and also to understanding their origination in relation with the laser processing parameters. Microstructure, phase constitution and mechanical properties of the ARTMCs were investigated by SEM, XRD and microhardness measurement.

2 Materials and experimental procedure

The following powders were used in the experiments: titanium powder was TiGd2 grade 99.76 wt% Ti (TLS Technik GmbH&Co). Micron size alumina powder was Aluminium Grenaille 350TL (Métaux & Chimie) and nano size alumina powder was ~15 nm (EvNanoTech.com. Ltd., China). Due to the nano dimensioned powder is impossible to transport through the coaxial nozzle with the gas flow, we mixed the nano dimensioned alumina with Ti powder in 1:1 ratio. The powder particles were mainly spherical with the size of ~80–100 μm for 95 % of them. The powder size distribution was studied by means of a granulomorphometer ALPAGA 500NANO (OCCHIO s.a.). The substrates were round plates with the 65 mm diameter and 5 mm height made of Ti-6Al-4 V.

All the experiments were carried out using a HAAS 2006D (Nd:YAG, 4000 W, cw) with the laser beam delivery system, powder feeding system, coaxial nozzle, and numerically controlled 5-axes table. Some features of the equipment are reported in (Shishkovsky and Smurov 2012).

The method of layerwise fabrication used in the present study was described thoroughly in (Shishkovsky et al. 2012) and is schematically presented in Fig. 1. Hatching distance was 2 mm, layer depth was ~1 mm, and the powder feeding rate was ~10 g/min. The layers were made out of Ti and Al_2O_3 powders on a substrate by the following strategy: the first layer was of titanium with 10 % Al_2O_3, the second one consisted of 80 % Ti + 20 % Al_2O_3, the third layer—of 70 % Ti + 30 % Al_2O_3. In the first case (strategy A) we used the micron size alumina powder. In the second case (strategy B) it was the Ti + nano Al_2O_3 mixture. Laser scanning speed was 500–750 mm/min, laser power varied within range of 800–1000 W, and laser beam diameter was 3 mm. The first channel feeder with the Ti powder had the gas flow rate of approximately 20 l/min while the second channel feeder with the Al_2O_3 (or Ti + nAl_2O_3) powder ~10 l/min.

It was necessary to select the etching agents for the prepared micro sections, ensuring of the basic structural phases being maximally reveal. For titanium aluminides, the aqueous solution of hydrofluoric and nitric acids taken in the equal portions was proved to be convenient, while for the Ti_xAl_y phases. After the etching, cross sections of the multi-layered cladding samples were subjected to metallurgical analysis with the optical microscope (Neophot 30 M, Carl Zeiss) equipped with a digital camera and a micro-hardness (HV) tester PMT-3 M (RF). The phase composition of the synthesized structures was determined with the x-ray diffraction (XRD) using a DRON-3 diffractometer in the Co-K_α radiation. The morphology of the laser cladded layers after the LMD was studied with a LEO 1450 scanning electron microscope (Carl Zeiss Company) equipped with an energy-dispersive x-ray analyzer (INCA Energy 300, Oxford Instruments).

3 Results and discussion

In accordance with the Ti–Al phase diagram we expected obtaining the following stable intermetallide phases of aluminium titanates—$TiAl_3$, TiAl, Ti_3Al during the in situ exothermic reaction of the type: x*Ti + y*Al → Ti_xAl_y + Q, where Q—is the additional

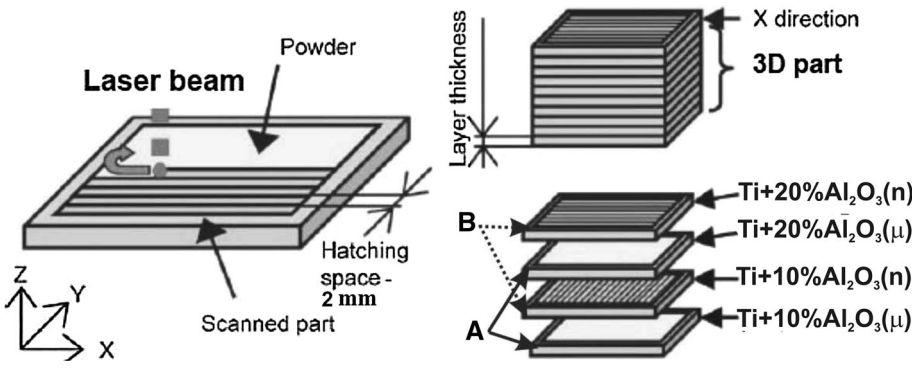

Fig. 1 Schematic of the multicomponent-graded structure fabrication in Ti–Al_2O_3 system by the LMD process of the ARTMC with: *A* micron and *B* nano sized alumina

thermal reaction effect. Under high temperature we expected Al releasing from alumina ceramic.

The results of optical metallography for μ- and n-ARTMC are presented in Fig. 2. Firstly, intensive pore and void formation during solidification should be noted for both the composite types. Moreover, the pores are distributed uniformly upon the height of the multilayers in the μ-ARTMC, while in n-ARTMC the pores are located predominantly near the remelted surface. Since the value of the laser energy input was approximately identical, we bind this difference with the high reactivity of the Al_2O_3 nano-particles and different wettability of μ- and n- alumina. The cracks between the layers are clearly visible in the Fig. 2a. The dot lines in Fig. 2a show the layer's boundaries roughly. This interfacial area has a heterogeneous character. A branched dendritic structure of columnar type with different orientation concerning heat dissipation should be noted in Fig. 2b in the case of n-Al_2O_3. A coarse structure with large grains of ~600…800 μm is clearly visible. It is interesting to remark that the nano-sized alumina with Ti can cause the formation of the fine dendrite structure; while the micro-sized counterpart cannot. In Fig. 2a a martensite morphology of the β-titanium phase is represented, and later it was supported by XRD and SEM results. The present structural heterogeneity is obviously connected with no uniform alloying, chaotic exothermal reactions of the intermetallic synthesis in the places of Ti and alumina particle contact and high-speed laser cooling during the crystallization after the melt. The top places of Fig. 2a were etched less clearly, so the dispersed precipitations of the second phase (α_2- Ti_3Al phase) appeared on their background. These intermetallic phases, being more durable, cause the crack development at the grain boundaries. Finally after the laser cladding, the upper layers had coarse elongated grains of dendrite type. By our opinion, the addition of the great quantity of oxide ceramic to "strengthen" the Ti alloy leads to the significant risk to decrease the final properties of the LMD-processed Ti alloy,

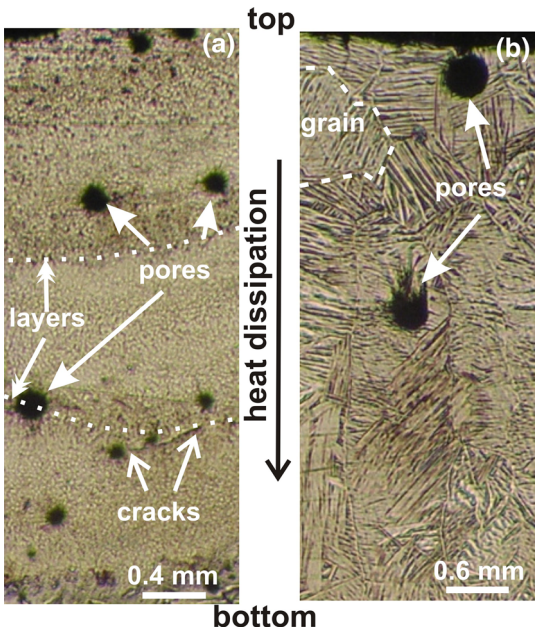

Fig. 2 OM micrographs showing the typical microstructures after LMD process in the ARTMC: **a** micron; **b** nano sized alumina

since the oxygen element involved has a considerably detrimental influence on the laser additive manufacturing process and quality of the Ti-based alloy.

The measured microhardness (Fig. 3) of the cladded layers grows from the substrate ($\sim$300 $HV_{0.1}$) to the top ($\sim$650 $HV_{0.1}$) irregularly. We believe this to be connected with a local hardness increase in the intermetallic phase locations. As a whole the microhardness values correspond to similar measurements on the titanium aluminides after the LMD and LENS processes (Shishkovsky et al. 2012).

The X-ray analysis results are presented in Fig. 4. As it is seen from the Fig. 4a, the most intensive lines belong to (110) TiO_2 and metastable $AlTi_2$ intermetallic phase. It is known that some basic peaks of the $AlTi_2$ phase can coincide with the diffraction lines of the $AlTi_3$ phase, which hampers their identification. The diffraction lines (110), (012) of the initial Al_2O_3 ceramic are clearly visible. Since the laser treatment was conducted in the protective environment of argon, the rutile (TiO_2 phase) presence should be connected with the oxygen release during the Al_2O_3 dissociation and is useful to enhance toughness and wear resistance of the sample (Wang et al. 2009). At the same time, the diffraction lines (101, 102, 110, 103, 201) of the initial titanium are quite numerous. Nevertheless the presence of not reacted Ti and even TiO_2 as foregoing cracks should be attributed to the unresolved problems of the discussed approach reinforced by the μ-alumina.

Figure 4b shows the X-ray analysis results after the LMD process in the n-ARTMC. Very strong peaks (201, 002, 202) of the $AlTi_3$ intermetallic phase are observed. There are also visible trails of not reacted titanium (100) and Al_2O_3. Moreover, in the view of crystallography, the rhombohedral corundum Al_2O_3 (04-0879, JCPDS, PCPDFWIN ver. 2.02 1999) in the Fig. 4b diffractogram differs from the XRD pattern of the Al_2O_3 (77-2135, JCPDS) in the Fig. 4a, which attests their different nature.

On taking into account all the peaks mentioned above, it's reasonable to conclude that this XRD pattern (Fig. 4) best of all coincides with the set of lines for the $AlTi_3$

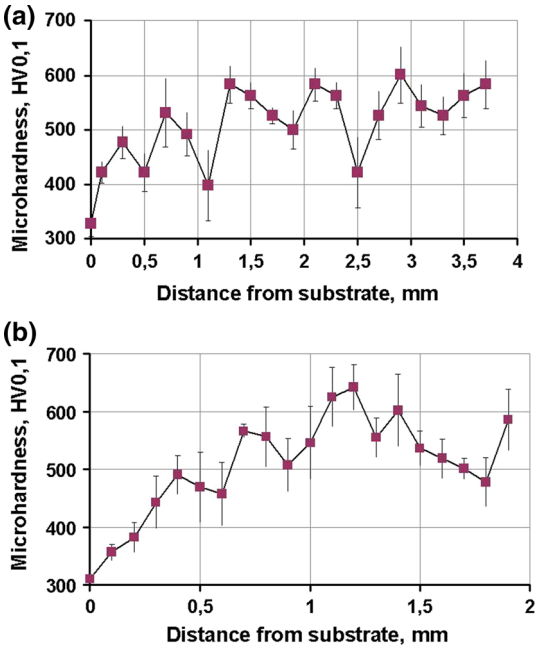

Fig. 3 Microhardness distributions of the ARTMC with: **a** micron and **b** nano sized alumina

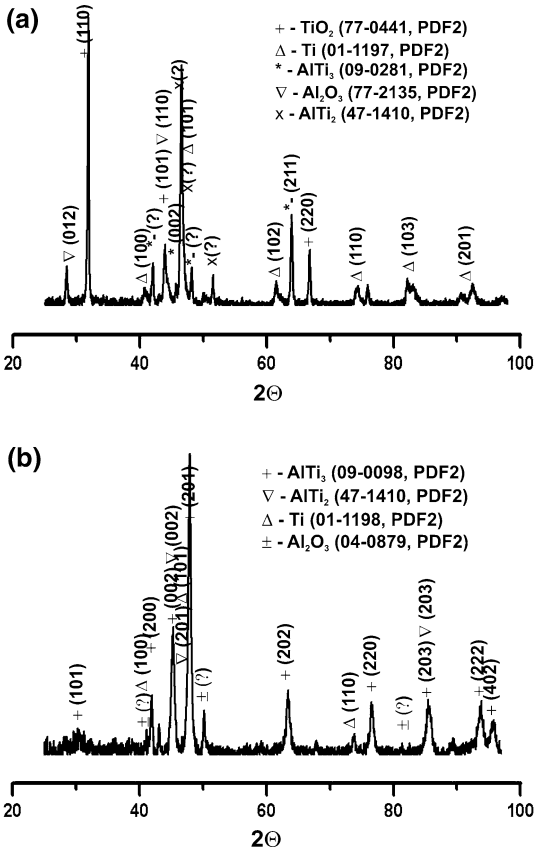

Fig. 4 X-ray diffraction patterns of the ARTMC with: **a** micron and **b** nano sized alumina

intermetallide. It means that the combustion reaction of the Ti_3Al intermetallic synthesis took place. This explains both the presence of a large number of residual non-reacted Ti powder and a very low quantity of pure alumina. Using of the nano-Al_2O_3 is more favourable for the intermetallic compound formation and answers the basic tasks of our study.

The SEM images of the substructures are shown in Fig. 5. In Fig. 5a, not completely reacted particles of Al_2O_3 are visible (F1—region) by the intermetallide grain boundaries (see also EDX results—D2 region). Their sizes ($\sim$1… 2 μm) are much less than the initial particle's size, which was $\sim$80 μm. In Fig. 5b we observe the intermetallide dendritic matrix. Heterogeneous character of the dendrite arrangement is similar to the optical microscopy data (Fig. 2b).

On the whole their images corresponded to the XRD data given above. The EDX data shows that, despite the fact we introduced up to 30 % of Al_2O_3, this alumina was practically not fixed. It is possible to suggest that temperature was enough to alumina decay.

Since the solid but brittle $AlTi_2$, $AlTi_3$ intermetallic phases identified by us as the initial μ-and n-alumina, are the second phase inclusions of the cladded layers in the titanium matrix, hence simultaneously with strengthening the titanium matrix, they cause its crack susceptibility. This was observed by us visually, though the middle layers with 20 % of alumina are preferred. Probably, with increasing Al_2O_3 content, significant cracking of the

(a)

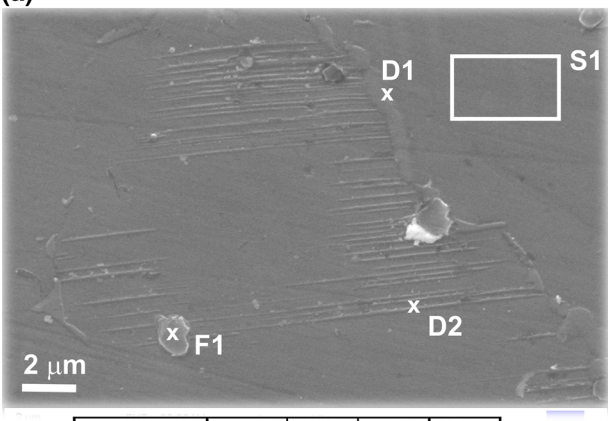

Element,.Wt%	Al K	Ti K	O K	Total
S1 area -	29.06	70.94	--	100.00
D1 point	30.22	69.78	--	100.00
D2 point	29.87	70.13	--	100.00
F1 particle	23.19	39.16	37.65	100.00

(b)

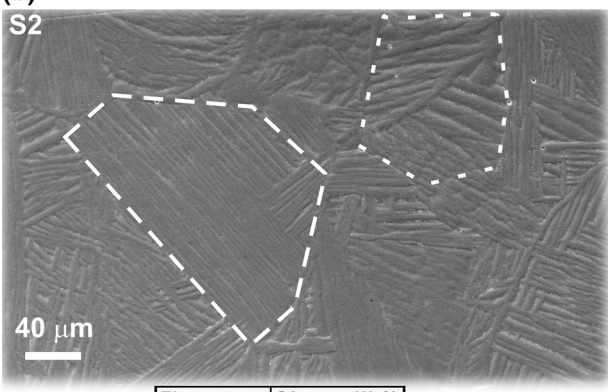

Element	S2 area - Wt %
Al K	12.94
Ti K	87.06
Total	100.00

Fig. 5 SEM micrographs showing typical solidification microstructures of clad coatings with the laser scanning speed of 500 mm/min and 1000 W with EDX results: **a** (S1, D1, D2 and F1 regions) of μARTMC; **b** (S12 region) of n-ARTMC

specimens occurred during remelting, due to increased CTE of the matrix (Shishkovsky and Smurov 2012). We agree with the suggestion made in the paper (Shishkovsky et al. 2012) that crack-free deposition and a porosity release can be achieved by preheating the substrate to 450–500 °C during the LMD process.

4 Conclusion

In the present study the multiphase ARTMC were fabricated in situ by LMD of Ti (10, 20, 30 wt%) μ- and n-Al_2O_3 powder mixtures by using laser with 1.064 mm wavelength operating at 1 kW power and at the laser scanning speed of 500–600 mm/min.

1. The single step LMD process was ensured to be a way of laser controlled synthesis of $AlTi_3$ intermetallic phase from the powder mixture Ti + (μ-/n-) Al_2O_3 and strengthening them as well as alumina of titanium matrix in itself.
2. Increase of microhardness from 300 to 600 HV was obtained within the same sample due to the change of the element relationship in the alumina-Ti system with 3D laser cladding.
3. All the samples contained pores but the lowest heterogeneity and cracking susceptibility after the laser solidification were achieved in middle layers with 20 % of alumina. In this case insignificant strengthening and practically porousless microstructure were observed due to using the nano size Al_2O_3 instead of the micron size.

Acknowledgments The study was supported by the grant of the Russian Foundation of Basis Researches (RFBR No. 14-29-10193 ofi-m).

References

Chen, Y., Wang, H.: Growth morphologies and mechanism of TiC in the laser surface alloyed coating on the substrate of TiAl intermetallics. J. Alloy. Compd. **351**, 304–308 (2003). doi:10.1016/S0925-8388(02)01077-0

Chen, Y., Wu, D., et al.: Coaxial laser cladding of Al_2O_3-13%TiO_2 powders on Ti-6Al-4 V alloy. Surf. Coat Techn. **228**, S452–S455 (2013). doi:10.1016/j.surfcoat.2012.05.027

Forouzanmehr, N., Karimzadeh, F., Enayati, M.: Synthesis and characterization of TiAl/α-Al_2O_3 nanocomposite by mechanical alloying. J. Alloy. Compd. **478**, 257–259 (2009). doi:10.1016/j.jallcom.2008.12.047

Gu, D., Shen, Y., Meng, G.: Growth morphologies and mechanisms of TiC grains during Selective Laser Melting of Ti–Al–C composite powder. Mater. Lett. **63**, 2536–2538 (2009a). doi:10.1016/j.matlet.2009.08.043

Gu, D., Wang, Z., et al.: In-situ TiC particle reinforced Ti–Al matrix composites: powder preparation by mechanical alloying and Selective Laser Melting behavior. Appl. Surf. Sci. **255**, 9230–9240 (2009b). doi:10.1016/j.apsusc.2009.07.008

Gu, D., Hagedorn, Y., et al.: Nanocrystalline TiC reinforced Ti matrix bulk-form nanocomposites by Selective Laser Melting (SLM): Densification, growth mechanism and wear behavior. Comp. Sci. Techn. **71**, 1612–1620 (2011). doi:10.1016/j.compscitech.2011.07.010

Krakhmalev, P., Yadroitsev, I.: Microstructure and properties of intermetallic composite coatings fabricated by selective laser melting of Ti-SiC powder mixtures. Intermetallics **46**, 147–155 (2014). doi:10.1016/j.intermet.2013.11.012

Li, J., Chen, C., Lin, Z., Tiziano, S.: Phase constituents and microstructure of laser cladding Al2O3/Ti3Al reinforced ceramic layer on titanium alloy. J. Alloy. Compd. **509**, 4882–4886 (2011). doi:10.1016/j.jallcom.2011.01.199

Li, J., Yu, H., et al.: Influence of Al_2O_3–Y_2O_3 and Ce–Al–Ni amorphous alloy on physical properties of laser synthetic composite coatings on titanium alloys. Surf. Coat. Techn. **247**, 55–60 (2014). doi:10.1016/j.surfcoat.2014.03.007

Shishkovsky, I., Smurov, I.: Titanium base functional graded coating via 3D laser cladding. Mater. Lett. **73**, 32–35 (2012). doi:10.1016/j.matlet.2011.12.099

Shishkovsky, I., Missemer, F., Smurov, I.: Direct metal deposition of functional graded structures in Ti-Al system. Phys. Procedia. **39**, 382–391 (2012). doi:10.1016/j.phpro.2012.10.052

Wang, D., Tian, Z., et al.: Influences of laser remelting on microstructure of nanostructured Al_2O_3–13 wt% TiO_2 coatings fabricated by plasma spraying. Appl. Surf. Sci. **255**, 4606–4610 (2009). doi:10.1016/j.apsusc.2008.11.082